Dynamic resonant tunneling via a quasibound superstate

Gilad Zangwill and Er'el Granot
Department of Electrical and Electronics Engineering, Ariel Photonics Center, Ariel University, Ariel 40700

(Received 10 June 2022; accepted 12 August 2022; published 1 September 2022)

The quantum tunneling current via an opaque barrier with an oscillating well reveals a wealth of physical phenomena: eigenstate-assisted activation, the elevator effect, coherent destruction of tunneling, suppression of activation, and the Sisyphus effect are a few examples. In this paper, we investigate these effects from a different perspective—transmission via a quasibound super state (QBSS). It is shown that an oscillating well supports a QBSS, which consists of numerous quasibound substates. Each one of these substates has a finite spectral width, which corresponds to the escape probability. However, they construct a unique spectrum, which consists of activated and suppressed quasi substates all of which are simultaneously excited. Thus, when the oscillating well is integrated into an opaque barrier, one can borrow an analogy from stationary resonant tunneling (RT). In the stationary RT scenario, current flows via a quasibound state. In the oscillating RT scenario, current flows via a QBSS. This analogy can easily explain many of the system's complex behaviors: the symmetry between the current's sensitivity to the incoming energy and the outgoing one, and even why some frequencies induce activation while others suppress it. This analogy can be applied to improve the sensitivity of the system when used for a frequency-controlled transistor for it predicts that when the incoming energy is shifted from the central resonance of the QBSS, the device's current becomes exponentially sensitive to the applied frequency. While the oscillations' frequency mainly determines the spectral distance between substates, the oscillations' amplitude determines the spectral width and center of the QBSS. Furthermore, it is suggested that this analogy can be applied to investigate microbiological systems (the olfactory system) and optical devices.

DOI: 10.1103/PhysRevA.106.032201

I. INTRODUCTION

A delta-function potential is often used as a model for a small quantum structure like atoms, point defects, or quantum dots. These "atom" models can be used in more complex structures such as lattices and resonant-tunneling (RT) systems [1–10]. In RT systems, quantum particles tunnel through an opaque barrier via a resonant quasibound state (QBS) [3,11–14]. The QBS's well can be conveniently modeled by a delta-function potential [15–21]. However, this convenience comes with a cost—due to the zero dimensions of this potential, a delta-function well can have only one bound state, and consequently, in an RT system, it can create only one quasibound state. Therefore, it cannot be used to simulate a multilevel system. However, there is at least one exception to this fundamental property. If the delta function oscillates, the bound state turns into a dynamic quasibound superstate. That is, instead of a single infinitely narrow energy level (bound state), the state is split into numerous quasibound substates. Each one of these substates has a finite spectral width due to its finite lifetime. All the substates are interconnected, and since some substates have positive energy, they have a finite probability to escape from the quasistate. However, if the well is deep enough then this probability can be arbitrarily small. Thus, in practice, the oscillating delta-function potential (ODFP) can support a superstate, which consists of multiple interacting states, with an arbitrary long lifetime. When the ODFP is placed in a barrier, the transmission through the barrier can be regarded in a way that was missed, to the best of our knowledge, in previous studies, namely: resonant tunneling via a quasibound superstate (QBSS).

Tunneling in the presence of oscillations exhibits an abundance of physical phenomena, which were studied for numerous purposes: to calculate the tunneling time [22], to study odorant-receptor interaction in the olfactory system [23–26], to study activation processes [16,17,27–30], and even tunneling and RT suppression in nanometric devices [15,18–21,31–36].

It was found that this relatively simple system reveals a wealth of physical phenomena much beyond expectations. It was expected that the oscillations would stimulate tunneling [16,17,22,27–29] and it would even be anticipated that an elevator effect would appear [16,17], i.e., that the incoming particle's energy can be elevated by the varying potential. Yet, the system's behavior exceeded expectations. It was found to be extremely sensitive to the incoming particle's energy and for certain energies, the tunneling current was considerably suppressed [15,18,19,34], while the suppression was explained as destructive interference between transition paths [15,18,33,34]. Similarly, certain energies are excluded from the outgoing particle's spectrum [15,18,19]. It should be noted that the spectral width of the excluded energies is exponentially narrow. The similarities between the sensitivity to the incoming particle's energy and the outgoing particle's spectra suggest that there is an inner structure, which deserves more research. Moreover, all the energy excitations are coupled, i.e.,

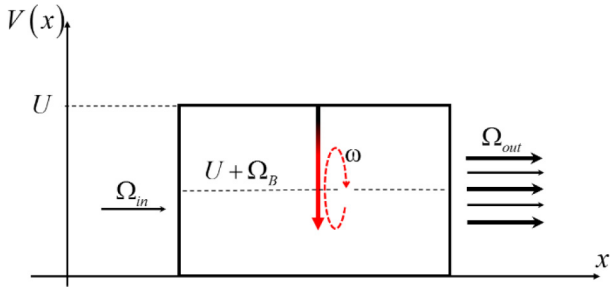

FIG. 1. The system under study. An energetic particle tunnels through an opaque barrier with an oscillating well at its center. The well oscillates with frequency ω. U is the barrier height, Ω_{in} is the incoming energy, and $U+\Omega_B$ is the central quasibound energy where Ω_B is defined by the well's parameters [Eq. (10)]. Ω_{out} is the outgoing energies (arrows' width indicates different transmission probabilities).

it is impossible to excite one without the other, while different energies are excluded.

The main object of this paper is to show that all these complicated behaviors can be attributed to the existence of a QBSS, and the current via a barrier with an oscillating well can be described as RT via a QBSS. As the usage of a quasibound state simplifies and explains the phenomenon of resonant tunneling, using the existence of a QBSS in a barrier can considerably simplify the understanding of all these complicated phenomena.

Therefore, in this paper, we take a different approach from the ones taken by us or others. First, while destructive interference can explain tunneling suppression, it cannot explain the coupling between the different excitations. Therefore, unlike other works, which investigated different temporal potential variations [15–18,37–39], in this research we focus on a harmonically oscillating potential to create spectrally split states as Floquet theory teaches [34,40]. Second, we *do not* follow the Floquet methodology. Instead of seeking a Floquet state, we investigate tunneling via the QBSS, which is not periodic and therefore *not* a Floquet state. Floquet states are stationary states of the system. The QBSS, on the other hand, is like a resonant state, i.e., it is a quasiunstable state, which does not have a real eigenenergy, and therefore *cannot be* a Floquet state. Third, since we aim to show that the QBSS presence is the cause of these effects, unlike Refs. [19,21,22,41] which directly solved a scattering problem, we first investigate the QBSS properties and only then do we incorporate it in an RT process. The presence of the QBSS as a physical entity was missed in previous studies.

The main claim is, therefore, that as the concept of tunneling via a resonant state simplifies the understanding of an RT process, the concept of tunneling via a QBSS simplifies considerably the understanding of the tunneling process via an oscillating potential well.

II. SYSTEM

The quantum system under study is presented in Fig. 1. The incoming particle hits an opaque barrier whose height is U and width is $2L$. At the center of the barrier, there is

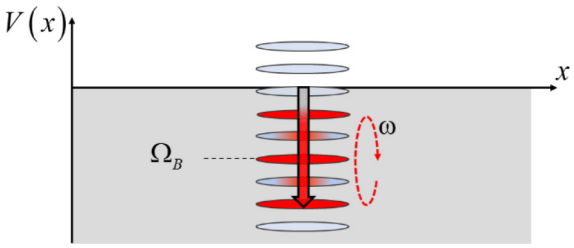

FIG. 2. An oscillating delta-function potential well supports a QBSS. ω is the oscillations' frequency and Ω_B is the central quasibound energy [Eq. (10)]. The QBSS's spectrum consists of multiple substates energies (11); some (red ones) are more excited than others (gray ones).

an oscillating well, which is modeled by an oscillating delta function. This system can be formulated using the following Schrödinger equation:

$$i\frac{\partial\psi}{\partial t}=-\frac{\partial^2}{\partial x^2}\psi+V(x)\psi+(\alpha+\beta\cos\omega t)\delta(x)\psi, \tag{1}$$

where the units were taken for convenience that the Planck constant is $\hbar=1$ and the particle's mass is $m=1/2$, and

$$V(x)=\begin{cases}U & |x|<L\\ 0 & else\end{cases}. \tag{2}$$

As was explained in the Introduction, we will first study the superstate that the oscillating well supports.

III. DYNAMIC QUASIBOUND SUPERSTATE

To investigate the superstate, we can omit the barrier, and study the eigenstates of the oscillating delta-function well (see Fig. 2). Therefore, the system can be formulated by a similar Schrödinger equation, but without the barrier [$V(x)=0$], i.e.,

$$i\frac{\partial\psi}{\partial t}=-\frac{\partial^2}{\partial x^2}\psi+(\alpha+\beta\cos\omega t)\delta(x)\psi. \tag{3}$$

Note that the well imposes that $\alpha<0$.

Since the potential is periodic, according to the Floquet theory [34], the states of the systems are periodic as well, and therefore can be written as a superposition of discrete energies' states. However, the quasibound-state solution of Eq. (3) $\Phi_B(x,t)$ is *not* a Floquet state. It is not a stationary-periodic state, but a dissipative one. When a particle is initially bounded to this potential it will eventually dissipate to the continuum by absorbing phonons' energy quanta. Only when the oscillations' frequency is considerably lower than the well's depth can this dissipation be neglected and $\Phi_B(x,t)$ can be written as a superposition of discrete energies as well, i.e.,

$$\Phi_B(x,t)=N\sum_{n=-\infty}^{\infty}t_n\exp\left(ik_n|x|-i\Omega_n t\right), \tag{4}$$

where $\Omega_n\equiv\Omega+n\omega$, $k_n\equiv\sqrt{\Omega_n}=\sqrt{\Omega+n\omega}$, and N is the normalization constant.

On the other hand, in the adiabatic regime, the particle's eigenstate must follow the potential's temporal changes, i.e.,

$$\frac{\Phi_B(x,t)}{N} \cong \exp\left[-\frac{(\alpha+\beta\cos\omega t)|x|}{2} + i\left(\frac{\alpha^2}{4}+\frac{\beta^2}{8}\right)t + i\frac{\alpha\beta}{2\omega}\sin\omega t + i\frac{\beta^2}{16\omega}\sin 2\omega t\right], \tag{5}$$

wherein this case the normalization constant satisfies $N = \sqrt{(\alpha+\beta\cos\omega t)/2}$. We will see below that since the probability to escape from the well is exponentially small, this adiabatic solution can be applied in a wide range of frequencies, provided the well is deep enough and the oscillations' amplitude is low enough. Therefore, for any frequency, one can find suitable well's parameters (α and β in this example) that allow using this approximation. Therefore, Eq.(5) can be used as a good approximation for the exact solution. To find the *numerical* solution, Eq. (4) should be substituted in (3) to receive the following difference equation for the coefficients t_n:

$$(\alpha - 2ik_n)t_n + \frac{\beta}{2}(t_{n+1}+t_{n-1}) \cong 0. \tag{6}$$

Such a solution exists provided the following determinant vanishes:

$$\begin{vmatrix} \ddots & \ddots & & & & & \\ \ddots & \alpha-2ik_{-2} & \beta/2 & & & & \\ & \beta/2 & \alpha-2ik_{-1} & \beta/2 & & & \\ & & \beta/2 & \alpha-2ik_0 & \beta/2 & & \\ & & & \beta/2 & \alpha-2ik_1 & \beta/2 & \\ & & & & \beta/2 & \alpha-2ik_2 & \ddots \\ & & & & & \ddots & \ddots \end{vmatrix} \cong 0. \tag{7}$$

Since the QBSS is not a Floquet state, there is no energy that solves Eq. (7) exactly but only approximately, i.e., for any finite matrix the states' energies are the minima of (7) (instead of its zeros).

Clearly, if Ω_B solves (7) then so does $\Omega_{B,n} = \Omega_B + n\omega$ because Eq. (6) does not depend separately on Ω and $n\omega$ but only on their combined term $\Omega + n\omega$. Therefore, we conclude that the QBSS has to consist of an infinite number of modes. Equation (7) can be rewritten to the second order of β as

$$1 - \left(\frac{\beta^2}{4}\right)\sum_{m=-\infty}^{\infty}\frac{1}{(\alpha-2ik_m)(\alpha-2ik_{m+1})} \cong 0. \tag{8}$$

Or, equivalently, for every m,

$$\frac{1}{(\alpha-2ik_m)(\alpha-2ik_{m+1})} + \frac{1}{(\alpha-2ik_{m-1})(\alpha-2ik_m)} \cong \frac{4}{\beta^2}. \tag{9}$$

The solution of Eq. (9), again up to the second order in β, is

$$\Omega_B \cong -\frac{1}{4}\left(\alpha^2+\frac{\beta^2}{2}\right), \tag{10}$$

and therefore, the generic solutions of (7) are

$$\Omega_{B,n} \cong \Omega_B + n\omega \tag{11}$$

for any integer n.

Correspondingly, the eigenvectors of Eq. (6) stand for the coefficients of the eigenstates of the QBSS. It should be noted that (10) is consistent with the time-independent part of the frequency of the adiabatic approximation of the QBSS (5). In the approximation where the oscillations' amplitude is weak in comparison to the well's depth, i.e., $\beta^2 \ll \alpha^2$ then (5) can be rewritten approximately,

$$\Phi_B(x,t) \cong \exp(-i\Omega_B t) \times \sum_{n=-\infty}^{\infty}\sqrt{\kappa_n}\exp(-\kappa_n|x| + in\omega t)(-1)^n J_n\left(\frac{\alpha\beta}{2\omega}\right), \tag{12}$$

where $\kappa_n \equiv \sqrt{-\Omega_B + n\omega}$ and $J_n(x)$ are Bessel functions of the first kind [42]. Equation (12) can be rewritten for simplicity in a more compact form as

$$\Phi_B(x,t) \cong 2\exp(-i\Omega_B t) \times \sum_{n=-\infty}^{\infty}\kappa_n^{3/2}G_{\Omega_{B,n}}(x)\exp(in\omega t)(-1)^n J_n\left(\frac{\alpha\beta}{2\omega}\right), \tag{13}$$

where

$$G_{\Omega_{B,n}}(x) = \frac{\exp\left(-\sqrt{-\Omega_{B,n}}|x|\right)}{2\sqrt{-\Omega_{B,n}}} \tag{14}$$

is the Green function of the stationary Schrödinger equation [Eq. (3)],

$$-\frac{\partial^2}{\partial x^2}G_{\Omega_{B,n}}(x) - \Omega_{B,n}G_{\Omega_{B,n}}(x) = \delta(x), \tag{15}$$

which means that the QBSS consists of infinite substates, each of which has a probability

$$p_n \sim |J_n(\alpha\beta/2\omega)|^2 \tag{16}$$

and the coefficients t_n should satisfy

$$t_n \cong J_n(\alpha\beta/2\omega). \tag{17}$$

In Fig. 3 we compare these coefficients to the exact solution.

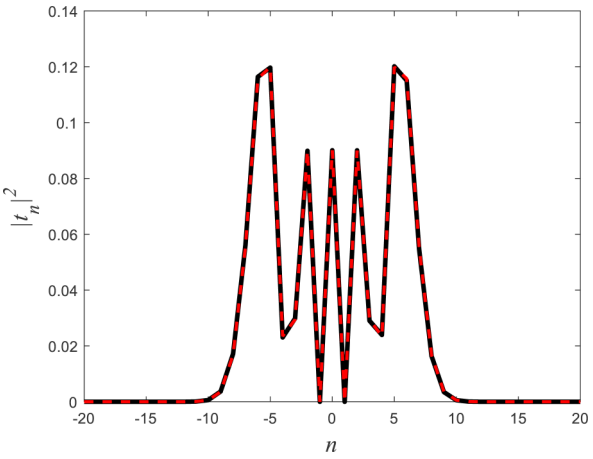

FIG. 3. Comparison between the slowly varying approximation Eq. (16) (dashed curved) to the exact solution (solid curve) of (6) for the parameters $\alpha/\sqrt{U} = -1.6$, $\beta/\sqrt{U} = 0.01$, and $\omega/U = 1.14 \times 10^{-3}$.

In the deep-well regime (i.e., adiabatic regime) many phonons have to be absorbed by the particle to be excited out of the well $[n \sim (\alpha^2/4 + \beta^2/8)/\omega \gg 1]$, and since for large n, $|J_n(z)|^2 \sim \frac{1}{2\pi n}(\frac{ez}{2n})^{2n}$, then the probability of escaping the well is exponentially small:

$$p_{\text{escape}} \sim \frac{2\omega}{\pi\alpha^2}\left(\frac{e\beta}{|\alpha|}\right)^{(\alpha^2/2\omega)}, \tag{18}$$

where e is Euler's number. Equation (18) is consistent with the premise that the adiabatic regime is valid provided the oscillations are weak in comparison to the well's depth. When this condition holds (i.e., $\omega \ll \alpha^2$), the probability to escape from the oscillating well is negligible, and the adiabatic approximation (5) is valid. Equivalently, the spectral width of the substates is on the order of $P_{\text{escape}}\alpha^2$. When the spectral distance between the subenergies is much larger than their width, i.e., $P_{\text{escape}}\alpha^2 \ll \omega$, the periodic adiabatic approximation is well defined, which, according to (18) holds when $\omega \ll \alpha^2$.

It should be noted that the transmission amplitudes $|t_n|^2$ are larger at the spectrum's edges (see Fig. 3) since these energies correspond to the well's maximum and minimum position, in which the well lingers the most.

IV. ELEVATED QUASIBOUND SUPERSTATE

Next, we add a barrier (2) and return to Eq.(1). It is therefore taken that the oscillating well is located at the center of a stationary barrier. Now the system still supports a QBSS. In this case, the bounded particle has another way of escaping from the well—it can tunnel out of it. When the barrier is very opaque, i.e., it is very wide or very high, the tunneling probability is negligible in comparison to the excitation probability, and therefore, there is no substantial difference in the spectral width of the substates, in which case the transmission through the barrier should reveal an exponentially large finesse:

$$finesse \sim \frac{\pi\alpha^2}{2}\left(\frac{\alpha}{e\beta}\right)^{(\alpha^2/2\omega)}. \tag{19}$$

However, as the barrier becomes more transparent the tunneling probability

$$p_{\text{tunnel}} \sim U\exp\left(-2\sqrt{U-\alpha^2/4}L\right) \tag{20}$$

becomes the main contributor to levels' spectral width, in which case the finesse decreases substantially,

$$finesse \sim \frac{\omega}{U}\exp\left(2\sqrt{U-\alpha^2/4}L\right). \tag{21}$$

Now Eq. (4) should be modified accordingly to

$$\Phi_{QB}(x,t) = \sum_{n=-\infty}^{\infty} t_n\varphi_n^+(|x|)\exp\left(-i\Omega_n t\right), \tag{22}$$

where $\varphi_n^{\pm}$ are the homogeneous solutions (when the well is absent) of the Schrödinger equation,

$$-\frac{\partial^2}{\partial x^2}\varphi_n^{\pm} + [V-\Omega_n]\varphi_n^{\pm} = 0, \tag{23}$$

which represent propagating waves through the barrier from left (right) to right (left), respectively. Therefore,

$$\varphi_n^+ \to \tau_{\Omega_n}\exp\left[ik_n x - i\Omega_n t\right] \text{ (for } x \to \infty), \tag{24}$$

$$\varphi_n^- \to \tau_{\Omega_n}\exp\left[-ik_n x - i\Omega_n t\right] \text{ (for } x \to -\infty), \tag{25}$$

and $|\tau_\Omega|^2$ is the probability to penetrate the barrier with energy Ω. Substituting (22) in (1), Eq. (6) can be replaced with

$$0 = (\alpha - \chi_n)s_n + \frac{\beta}{2}(s_{n+1} + s_{n-1}), \tag{26}$$

where $s_n \equiv t_n(\varphi_n^+/\varphi_0^+)$ and $\chi_n \equiv \frac{\varphi_n^+}{\varphi_n^+} - \frac{\varphi_n^-}{\varphi_n^-} = \frac{1}{g_n(0)}$, where $g_n(0) = -\frac{\coth[\rho_n L + i\arctan(k_n/\rho_n)]}{2\rho_n}$ is the Green function at $x = 0$ [15,19], and $\rho_n = \sqrt{U-\Omega_n}$.

The ratio φ_n^+/φ_0^+ can be written explicitly:

$$\frac{\varphi_n^+(0)}{\varphi_0^+(0)} = \frac{1+r_n}{1+r_0} = \frac{1+\exp\left[-2\rho_n L + 2iatan(k_n/\rho_n)\right]}{1+\exp\left[-2\rho_0 L + 2iatan(k_0/\rho_0)\right]}. \tag{27}$$

In the case of an opaque barrier, the QBSS can now be approximated by

$$\Phi_B(x,t) \cong 2\exp\left[-i(U+\Omega_B)t\right] \times \sum_{n=-\infty}^{\infty}\Omega_{B,n}^{3/4}G_{U+\Omega_B+n\omega}\exp\left(in\omega t\right)(-1)^n J_n\left(\frac{\alpha\beta}{2\omega}\right), \tag{28}$$

because, when the barrier is very opaque, the QBSS keeps its form for a very long period, albeit it may be considerably shorter than in the case where the barrier was missing and most of the substates had negative energies. Now, these resonances energies, which correspond to the quasisubstates' energies are approximately

$$\Omega_R \sim U + \Omega_B + n\omega \cong U - \frac{1}{4}\left(\alpha^2 + \frac{\beta^2}{2}\right) + n\omega. \tag{29}$$

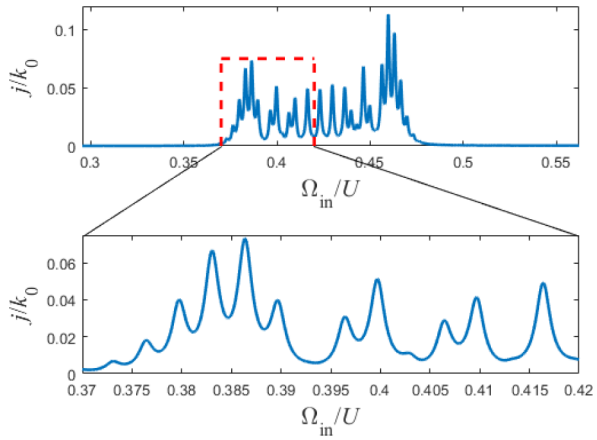

FIG. 4. Current through the barrier as a function of the incoming particle's energy. The numerical parameters are $\beta/\sqrt{U} = 0.1$, $\alpha/\sqrt{U} = -2.63$, $\omega/U = 0.01$, $L\sqrt{U} = 3$, and $U = 3$.

V. RESONANT TUNNELING VIA THE QBSS

Next, we address the RT scenario, i.e., the case where an incident particle hits the barrier with a given energy Ω. The wave function then can be written as

$$\psi(x,t) = \begin{cases} \varphi_0^+ \exp(-i\Omega_0 t) + \sum_{n=-\infty}^{\infty} r_n \varphi_n^- \exp(-i\Omega_n t) & x < 0 \\ \sum_{n=-\infty}^{\infty} t_n \varphi_n^+ \exp(-i\Omega_n t) & x > 0 \end{cases}, \tag{30}$$

wherein this case the difference equation reads

$$-\chi_n \delta(n) = (\alpha - \chi_n) s_n + \frac{\beta}{2}(s_{n+1} + s_{n-1}) \tag{31}$$

and the current through the barrier is

$$j = \sum_{n=-\infty}^{\infty} |t_n|^2 |\tau_n|^2 k_n. \tag{32}$$

The current as a function of the incoming particle's energy is plotted in Figs. 4 and 5. The resonances are clearly seen. Moreover, the wider the barrier, the narrower the spectral peaks.

Clearly, the spectra are not symmetric because particles with higher energy can tunnel more easily through the barrier. When the coefficients themselves are presented as a function of the incoming energy, the symmetry reappears. Not only do we see the symmetry between high and low energy (in comparison to the resonance energy Ω_R) but there is a clear symmetry between Ω_{in} and Ω_{out}. This picture is consistent with the excitation of the QBSS. All the substates are interconnected, and therefore they cannot be excited separately. Therefore, the probability that an incoming plane wave with energy Ω_{in}, i.e., the state $|\Omega_{in}\rangle$, will excite the QBSS $|\Phi_{QB}\rangle$ is

$$p_{ex} \sim |\langle \Omega_{in} \mid \Phi_{QB} \rangle|^2. \tag{33}$$

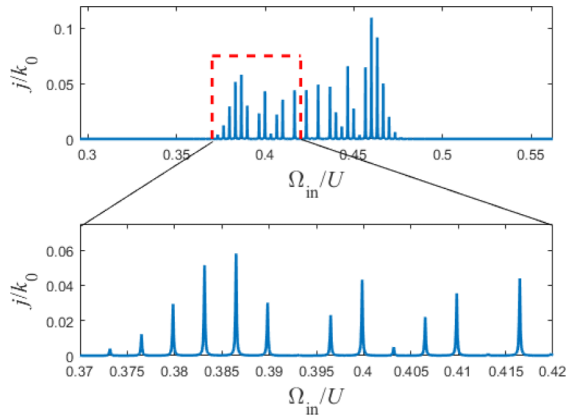

FIG. 5. Same system as Fig. 4, but with a wider barrier ($L\sqrt{U} = 4$).

And, the probability of the QBSS tunneling out of the barrier with energy Ω_{out} to the free state $|\Omega_{out}\rangle$ is

$$p_{tun} \sim |\langle \Phi_{QB} \mid \Omega_{out} \rangle|^2. \tag{34}$$

Therefore, the probability of an incoming particle with energy Ω_{in} tunneling out with energy Ω_{out} is

$$p_{\Omega_{in},\Omega_{out}} \sim |\langle \Omega_{in} \mid \Phi_{QB} \rangle|^2 |\langle \Phi_{QB} \mid \Omega_{out} \rangle|^2. \tag{35}$$

In the case of a deep well, this expression can be approximated by

$$p_{\Omega_{in},\Omega_{out}} \sim \left| J_n\left(\frac{\alpha\beta}{2\omega}\right) J_m\left(\frac{\alpha\beta}{2\omega}\right) \right|^2, \tag{36}$$

where $n = (\Omega_{in} - \Omega_R)/\omega$ and $m = (\Omega_{out} - \Omega_R)/\omega$.

Equation (36) is consistent with Fig. 6.

One of the clear conclusions from (36) is that the excited substates are

$$-\frac{\alpha\beta}{2\omega} < m < \frac{\alpha\beta}{2\omega},$$

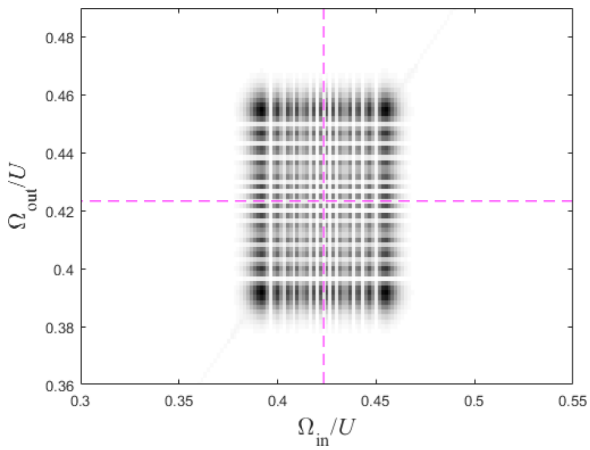

FIG. 6. Transmission coefficients $|t_n|^2$ as a function of the incoming and outgoing energies. The darker the color, the higher the probability value. The dashed line represents the resonance energy value Ω_R. The parameters are as in Fig. 5.

which means that the QBSS consists of approximately $\alpha\beta/\omega$ substates. Therefore, since the spectral distance between substates is ω, then the spectrum of the QBSS is $\Delta\Omega \sim \alpha\beta$, which is consistent with the "particle" picture, in which the particle's energy varies with the bound energy of the varying well, i.e., the change is difference between the maximum $-(\alpha-\beta)^2/4$ and minimum $-(\alpha+\beta)^2/4$ values of the quasibound state. As was explained above, at these maximum and minimum energies of the spectrum the well lingers the most and therefore the transmission energies are higher.

VI. SUPPRESSED STATES

The probability to excite the QBSS $p_{\rm ex}$ can be used to calculate the energies in which activation is suppressed. According to (36) the energies for which the Bessel function vanishes are the ones that suppress tunneling. In the regime of low oscillations frequencies, the Bessel function can be approximated by $J_n(z) \sim \sqrt{2/\pi z}\cos(z-n\pi/2-\pi/4)$ [42], and therefore the suppression occurs for

$$\Omega_{\rm in} = \Omega_m^* \text{ for } m = 0, \pm1, \pm2, \ldots, \tag{37}$$

when

$$\Omega_m^* \cong U - \left(\frac{\alpha^2}{4} + \frac{\beta^2}{8}\right) \pm \left[\frac{|\alpha|\beta}{\pi} - 2\omega\left(m + \frac{3}{4}\right)\right]. \tag{38}$$

These suppression energies are consistent with Refs. [15,18], where a generic expression was derived for suppressing energies, namely

$$\int_0^{t_1} \{E - [U - \Omega_B(t')]\}dt' = \left(m - \tfrac{1}{4}\right)\pi, \tag{39}$$

wherein this case $\Omega_B(t) \equiv (\alpha + \beta\cos\omega t)^2/4$, and since $E \cong \Omega_R$ then $t_1 \cong \pi/2\omega$. It should be stressed that in Refs. [15,18] the QBSS was not even discussed. Equation (38) is an excellent approximation at the vicinity of the center of the spectrum, but for energies far from the center of the spectrum, this approximation is no more valid and at the edges of the spectrum we suggest a different approximation: Since the quasibound energy $\Omega_B(t)$ oscillates, it has a minimum and maximum energy (both lower than the barrier height). By approximating these minimum (maximum) curves to a parabola, we find the energies at which activation is suppressed:

$$\Omega_m^{\pm} = U - \frac{1}{4}(\beta \mp \alpha)^2 \pm \left(\beta^2 - \alpha\beta\right)^{1/3}\left[\frac{3\omega}{4}\left(m + \frac{3}{4}\right)\pi\right]^{2/3}. \tag{40}$$

Equation (40) is consistent with Refs. [15,18,19] and shows excellent agreement with the numerical results.

In Fig. 7, the logarithm of the current [$\ln(J)$] as a function of the incoming energy $\Omega_{\rm in}$ and as a function of the vibrations' amplitude β, is presented (exact numerical solution). The larger the amplitude β, the wider the spectrum. Black spots represent high current while white spots represent low current. In the right figure [Fig. 7(b)], the analytical solutions are presented above the numerical solution: the red dashed curves represent Eq. (40) (for) $m = 0$ and $m = 1$ and the dotted red curves represent the solutions of Eq. (38) (for) $m = 2$ and $m = 3$. There is an excellent agreement between the approximated analytical results and the exact numerical results.

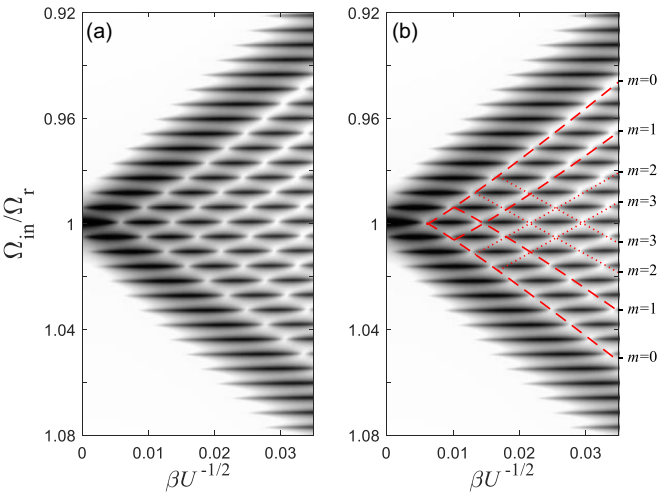

FIG. 7. Outgoing current as a function of the incoming energy $\Omega_{\rm in}/\Omega_r$ and as a function of the vibrations' amplitude β, where $\Omega_r = U - \alpha^2/4$. The darker the color, the higher the current. (a) stands for the numerical solution. (b) The approximate analytical solutions are presented above the numerical solution. The dashed curves represent Eq. (40) for $m = 0$ and $m = 1$ and the dotted curves represent the solutions of Eq. (38) for $m = 2$ and $m = 3$. The parameters are $U = 1$, $L\sqrt{U} = 6$, $\alpha/\sqrt{U} = -1.6$, and $\omega/U = 0.002$.

In Fig. 8 we present the same parameters as in Fig. 7 but for a larger range of amplitudes and a narrower spectrum range. One of the purposes of this graph is to show the square dependency of the resonance energy Ω_R on the vibrations' amplitude β.

In a stationary scenario where the coefficient of the delta-function potential is time independent (i.e., $\beta = 0$), the quasibound energy is simply $\Omega_r = U - \alpha^2/4$, and there is only one specific quasibound state, but when the potential

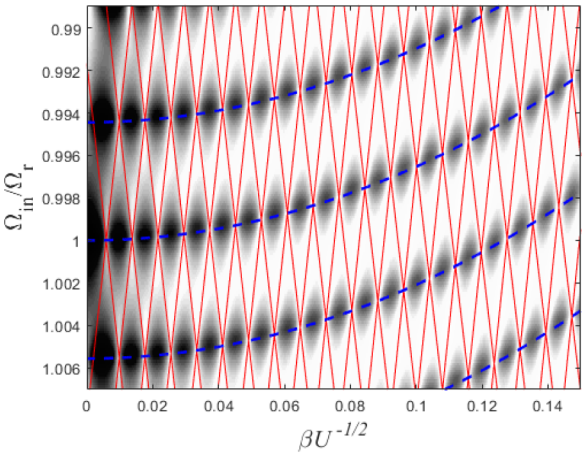

FIG. 8. Outgoing current as a function of the incoming energy $\Omega_{\rm in}$ and the vibrations' amplitude β. The darker the color, the higher the current. Equation (29) is presented by blue dashed curves and Eq. (38) is presented by red curves. The parameters are the same as in Fig. 7.

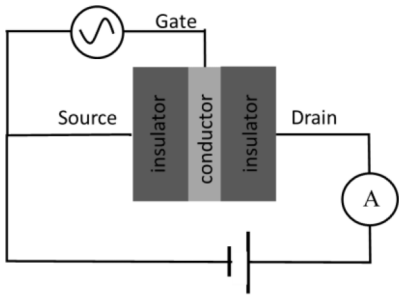

FIG. 9. Frequency-controlled transistor schematic. A conducting layer (the well in our model) is sandwiched between two insulators (barriers). The conductor can be a semiconductor or a metal layer and the insulators can be oxide or semiconductor layers. An external gate controls the well's oscillations. The whole device can be a few nanometers wide.

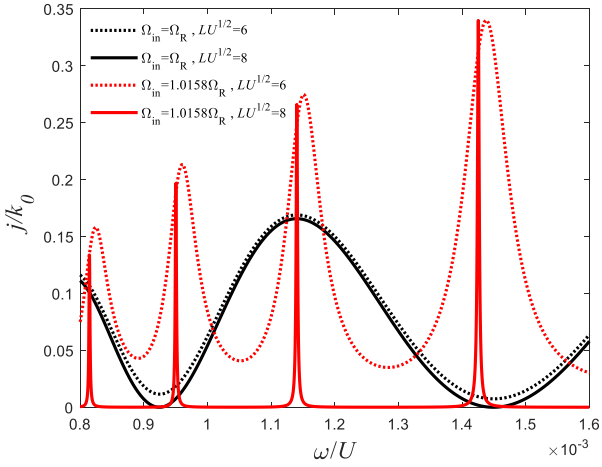

FIG. 10. Output current as a function of the oscillation frequency ω for two different inputs. The black curves correspond to the input energy $\Omega_{\text{in}} = \Omega_R$ (the central resonance energy) and the red curves represent the input energy $\Omega_{\text{in}} = 1.0158 \cdot \Omega_R$. The solid curves represent the case $L\sqrt{U} = 8$ and the dotted curves correspond to the case where the barrier width is $L\sqrt{U} = 6$. The other parameters are $U = 1$, $\alpha/\sqrt{U} = -1.6$, and $\beta/\sqrt{U} = 0.01$.

oscillates with amplitude β and frequency ω, the resonance energy is shifted proportionally to β^2, and the single quasibound state splits into interconnected substates which the superstate consists of. Equation (29) is an approximate formula that describes the shift in energy and the splitting into a superstate. Equation (29) is presented in Fig. 8 by blue dashed curves. Since we exhibit only a narrow spectral width around the center of the spectrum, Eq. (38) gives excellent results for any amplitude β. The suppressed energies [Eq. (38)] are presented in red curves. There is an excellent agreement between the exact numerical results and the approximated analytical results.

VII. DISCUSSION AND APPLICATIONS

It has been shown above that when the well oscillates a QBSS is generated, and the transmission via a barrier with the oscillating well can be interpreted as RT via a QBSS. By using this analogy a better intuition can be developed, which simplifies the understanding of these complicated processes. Moreover, the intuition which is developed by the QBSS can be used to develop dynamic quantum and optical devices. In what follows we use the QBSS properties in a quantum device, in an optical device, and even in a quantum-biological system.

A. High-precision frequency-controlled transistor

As was discussed in the previous sections, the QBSS consists of interconnected multiple quasilevels. This property can be utilized to design an extremely sensitive transistor. In such a device the current is controlled by the frequency of the oscillations. Since frequency can be modified with great precision (much higher than possible with voltage or currents), this transistor can exhibit superior performances over state-of-the-art ones. Furthermore, the depth of the well (or the particles' Fermi energy) can be modified to reach the optimized sensitivity.

It has been suggested before to use oscillating well as a controller for a frequency-controlled transistor (see Fig. 9); however, the QBSS analysis gives an added value. It teaches that it is worthwhile to create a spectral shift between the well's depth and the particles' Fermi energy. In previous works [15,18–20], the analysis of such a device was focused on the central energy of the QBSS $\Omega_{\text{in}} = \Omega_R$. In this case, the well's frequency determines whether there will be destructive or constructive interference. However, the QBSS analysis reveals an insight that while the spectral width of the quasisubstates varies with the frequency, the central energy does not. Therefore, if the Fermi energy is higher (lower) than the central energy, then the system becomes more sensitive to the frequency because an exponentially small change suppresses the system's resonance. This point was missing in previous works on these systems. In Fig. 10 this fine sensitivity is illustrated. When the energy of the incoming particle (the Fermi energy) is equal to the central energy $\Omega_{\text{in}} = \Omega_R$, then the system has a mild dependence on the well's frequency and has no dependence on the barrier's opaqueness. However, when there is an energy shift between the well's eigenenergy and the incoming particle's energy, the current becomes much more sensitive to frequency variations, and the sensitivity is related to the resonances' spectral width, which depends exponentially on the barrier's width. Therefore, this property can be used to improve the transistor's sensitivity and precision.

B. QBSS in odor-receptor mechanism

There are several pieces of evidence that indicate that the biological olfactory system is based on a dynamic RT mechanism [23–26]. The biological olfactory system distinguishes between an enormous number of molecules using a relatively small number of different receptors (about a few hundred different receptors in most mammals) [43,44]. A specific odorant can activate multiple receptors, and a specific receptor can be activated by multiple molecules. Thus, different molecules trigger a different combination of receptors [44,45]. The mechanism by which a molecule triggers a receptor is not well understood and is usually described by two major theories: the docking theory [46,47], and the vibration theory

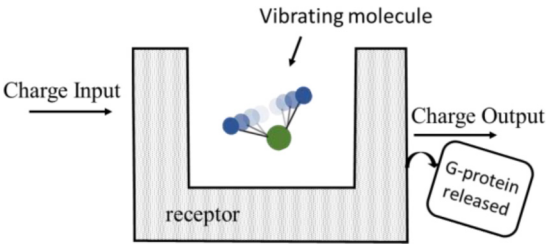

FIG. 11. Odor receptor schematic. To activate the receptor, electrons must tunnel across the receptor's structure (the barriers in our model). The tunneling current leads to the release of a G protein for further interactions. Only specific odorants (the well in our model) with specific vibrational frequencies (ω) will activate any given receptor.

[23,24]. Reference [23] suggests that the interaction between odorant and receptor is governed by a quantum tunneling mechanism (see Fig. 11). According to this model, the receptor functions as a potential barrier with an excess charge on one side of the barrier. When a molecule vibrates inside the receptor with an appropriate frequency, the charge can flow across the barrier while losing energy quanta causing receptor activation. While this model may be valid, it cannot explain the receptor's ability to distinguish between so many odors, since in this model the receptor's response is binary (either activated or not).

The QBSS model may give a better presentation of the problem because it shows that every combination of a receptor and a molecule has a distinct QBSS, i.e., different dependence on the incoming/outgoing particle's energy. Consequently, the different receptors can reconstruct the molecule's fingerprint by measuring simultaneously different parts of the QBSS spectrum.

C. Optical analogy

The mathematical analogy between the Schrödinger equation and the slowly varying Maxwell's equation can be used to apply the QBSS analysis to the optical domain. When light propagates through layers with different refractive indexes with an incident angle larger than the critical angle, then for specific cases total internal reflection vanishes and the light is fully transmitted through the layers as in the quantum resonant tunneling equivalent [48]. The discussion above suggests that an equivalent tunneling via a QBSS will appear in an optical device, where the middle layer's refractive index oscillates. Therefore, in analogy to the quantum scenario, the incident plane-wave electromagnetic field can be written:

$$\mathbf{E}(x,y) = \hat{z}A(x,t)\exp\left[i(k_y y - \omega t)\right], \tag{41}$$

where the slowly varying amplitude $A(x,t)$ satisfies the following equation:

$$-\frac{\partial^2}{\partial x^2}A + \left[k_y^2 - k_0^2 n^2(x)\right]A = \frac{n_0^2 2i\omega}{c^2}\frac{\partial}{\partial t}A, \tag{42}$$

where we assumed that the variation in the index of refraction is negligible in comparison to the ratio between the oscillations' frequency ω_0 and the optical frequency ω:

$$n^2(x) = n_0^2 + \Delta n^2 w[1 + m\cos(\omega_0 t)]\delta(x), \tag{43}$$

where w is the width of the thin middle layer, Δn is the change in its refractive index, and $m \ll 1$ is the modulation depth. Using the parameter $\tau \equiv \frac{c^2}{n_0^2 2\omega}t$, Eqs. (42) and (43) can be rewritten as

$$-\frac{\partial^2}{\partial x^2}A + \left[k_y^2 - k_0^2 n^2(x,\tau)\right]A = i\frac{\partial}{\partial \tau}A \tag{44}$$

and

$$k_0^2 n^2(x,\tau) = k_0^2 n_0^2 + \left[\alpha + \beta\cos\left(\omega_0 \frac{2n_0^2\omega}{c^2}\tau\right)\right]\delta(x), \tag{45}$$

respectively.

Since in this case $\alpha = k_0^2\Delta n^2 w$, $\beta = k_0^2 m\Delta n^2 w$, and the effective frequency is $\tilde{\omega} \equiv 2n_0^2\omega_0\omega/c^2$, the transmission of the nth substate is then

$$T_n \sim |J_n(\alpha\beta/2\tilde{\omega})|^2 = \left|J_n\left[\left(k_0^2\Delta n^2 w\right)^2 c^2 m/4n_0^2\omega\omega_0\right]\right|^2. \tag{46}$$

Since the number of excited submodes is $\alpha\beta/\tilde{\omega}$ the spectral widening is then

$$\Delta\omega \sim \left(k_0\Delta n^2 w\right)^2 \omega m/2n_0^2. \tag{47}$$

Consequently,

$$\frac{\Delta\omega}{\omega} \sim \frac{m}{2}\left(k_0 w\frac{\Delta n^2}{n_0}\right)^2. \tag{48}$$

This result is independent of oscillating frequency ω_0. Since in the optical regime $\omega \sim 10^{14}$Hz, then even though the right-hand side of Eq. (48) is smaller than 1, the spectral widening, which can be measured easily with optical spectrometers, can be widened by orders of magnitude, for example, using a $LiNbO_3$ (LNO), which has an unclamped Pockels coefficient of $r_{51} = 33\,\mathrm{pm/V}$ [49], Then, with a modulation depth of $m = 0.001$ one can increase sub-kHz modulation by six orders of magnitude to a few GHz.

VIII. SUMMARY

In this paper, it has been suggested to borrow the tools that were originally developed for stationary RT and apply them to explain the complex behavior of quantum current which passes via an opaque barrier with an oscillating well. An oscillating well creates a QBSS with a unique spectrum corresponding to the oscillation's parameters. This spectrum consists of activated substates and suppressed substates. Since all these quasisubstates are interconnected, they can be regarded as a QBSS. Therefore, as the sensitivity of an RT device can be interpreted in terms of the spectral proximity between the incoming particle's energy and the quasibound-state eigenenergy, the complexity of the system under discussion can be interpreted in a view of the matching between the incoming particle's energy and the QBSS's spectrum. It is shown that this view of the system can easily explain most of the complex behaviors of the system [e.g., selective activation (suppression)]. Moreover, the QBSS model can be used to improve the sensitivity of a frequency-controlled transistor,

which is based on an oscillating RT device. Furthermore, the QBSS can be used to simplify complex quantum-biological systems (e.g., olfactory system), and can be implemented in equivalent optical systems and devices.

[1] A. A. Frost, Delta-Function Model. I. Electronic energies of hydrogen-like atoms and diatomic molecules, J. Chem. Phys. **25**, 1150 (1956).

[2] R. de L. Kronig and W. G. Penney, Quantum mechanics of electrons in crystal lattices, Proc. R. Soc. London, Ser. A **130**, 499 (1931).

[3] M. Razavy, *Quantum Theory of Tunneling* (World Scientific, Singapore, 2003).

[4] E. Demiralp and H. Beker, Properties of bound states of the Schrödinger equation with attractive Dirac delta potentials, J. Phys. A **36**, 7449 (2003).

[5] G. Kalbermann, Assisted tunneling of a metastable state between barriers, Phys. Rev. C **77**, 041601(R) (2008).

[6] S. Geltman, Bound states in delta function potentials, J. At., Mol., Opt. Phys. **2011**, 573179 (2011).

[7] G. T. Camilo, F. A. Barone, and F. E. Barone, Interactions between delta-like sources and potentials, Phys. Rev. D **87**, 025011 (2013).

[8] M. Belloni and R. W. Robinett, The infinite well and Dirac delta function potentials as pedagogical, mathematical and physical models in quantum mechanics, Phys. Rep **540**, 25 (2014).

[9] A. Tanimu and E. A. Muljarov, Resonant states in double and triple quantum wells, J. Phys. Commun. **2**, 115008 (2018).

[10] A. A. Elkamshishy and C. H. Greene, Observation of Wigner-Dyson level statistics in a classically integrable system, Phys. Rev. E **103**, 062211 (2021).

[11] D. Bohm, *Quantum Theory* (Dover Publications, New York, 1989).

[12] L. Esaki and R. Tsu, Superlattice and negative differential conductivity in semiconductors, IBM J. Res. Dev. **14**, 61 (1970).

[13] L. L. Chang, L. Esaki, and R. Tsu, Resonant tunneling in semiconductor double barriers, Appl. Phys. Lett. **24**, 593 (1974).

[14] A. Belkadi, A. Weerakkody, and G. Moddel, Demonstration of resonant tunneling effects in metal-double-insulator-metal (MI^2M) diodes, Nat. Commun **12**, 2925 (2021).

[15] E. Granot and G. Zangwill, Dynamic resonant tunneling, in *Quantum Dynamics*, edited by P. Bracken (InTech, Rijeka, Croatia, 2016), p. 55.

[16] M. Y. Azbel, Elevator resonance activation, Europhys. Lett. **18**, 537 (1992).

[17] M. Y. Azbel, Eigenstate Assisted Activation, Phys. Rev. Lett **68**, 98 (1992).

[18] G. Zangwill and E. Granot, Eigenstate suppressed activation, Physica B **461**, 140 (2015).

[19] E. Granot, Selected elevation in quantum tunneling, Europhys. Lett. **61**, 817 (2003).

[20] G. Zangwill and E. Granot, Spatial vibrations suppressing resonant tunneling, Phys. Rev. A **101**, 012109 (2020).

[21] E. Granot, The tunneling current through oscillating resonance and the Sisyphus effect, Adv. Condens. Matter Phys. **2017**, 2435857 (2017).

[22] M. Büttiker and R. Landauer, Traversal Time for Tunneling, Phys. Rev. Lett. **49**, 1739 (1982).

[23] L. Turin, A spectroscopic mechanism for primary olfactory reception, Chem. Senses **21**, 773 (1996).

[24] J. C. Brookes, F. Hartoutsiou, A. P. Horsfield, and A. M. Stoneham, Could Humans Recognize Odor by Phonon Assisted Tunneling? Phys. Rev. Lett. **98**, 038101 (2007).

[25] M. I. Franco, L. Turin, A. Mershin, and E. M. C. Skoulakis, Molecular vibration-sensing component in drosophila melanogaster olfaction, Proc. Natl Acad. Sci. USA **108**, 3797 (2011).

[26] S. Gane, D. Georganakis, K. Maniati, M. Vamvakias, N. Ragoussis, E. M. C. Skoulakis, and L. Turin, Molecular vibration-sensing component in human olfaction, PLoS ONE **8**, e55780 (2013).

[27] A. Zangwill and P. Soven, Resonant Photoemission in Barium and Cerium, Phys. Rev. Lett. **45**, 204 (1980).

[28] B. I. Ivlev and V. I. Mel'nikov, Stimulation of Tunneling by a High-Frequency Field: Decay of the Zero-Voltage State in Josephson Junctions, Phys. Rev. Lett. **55**, 1614 (1985).

[29] M. P. A. Fisher, Resonantly enhanced quantum decay: A time-dependent Wentzel-Kramers-Brillouin approach, Phys. Rev. B **37**, 75 (1988).

[30] G. Platero and R. Aguado, Photon-assisted transport in semiconductor nanostructures, Phys. Rep. **395**, 1 (2004).

[31] M. Wagner, Quenching of resonant transmission through an oscillating quantum well, Phys. Rev. B **49**, 16544 (1994).

[32] M. Wagner, Photon-assisted transmission through an oscillating quantum well: A transfer-matrix approach to coherent destruction of tunneling, Phys. Rev. A **51**, 798 (1995).

[33] Y. Kayanuma, Role of phase coherence in the transition dynamics of a periodically driven two-level system, Phys. Rev. A **50**, 843 (1994).

[34] M. Grifoni and P. Hänggi, Driven quantum tunneling, Phys. Rep. **304**, 229 (1998).

[35] L. J. Lauhon and W. Ho, Direct Observation of the Quantum Tunneling of Single Hydrogen Atoms with a Scanning Tunneling Microscope, Phys. Rev. Lett. **85**, 4566 (2000).

[36] A. Ben-Asher, D. Šimsa, T. Uhlířová, M. Šindelka, and N. Moiseyev, Laser Control of Resonance Tunneling Via an Exceptional Point, Phys. Rev. Lett. **124**, 253202 (2020).

[37] M. Ya. Azbel, Resonances and oscillations in tunneling in a time-dependent potential, Phys. Rev. B **43**, 6847 (1991).

[38] J. Campbell, Some exact results for the Schrödinger wave equation with a time-dependent potential, J. Phys.A Math. Theor. **42**, 365212 (2009).

[39] E. Granot, Forbidden activation energies in non-stationary tunneling process, Physica E **14**, 397 (2002).

[40] D. F. Martinez and L. E. Reichl, Transmission properties of the oscillating δ-function potential, Phys. Rev. B **64** 245315 (2001).

[41] A. S. Stone, M. Ya. Azbel, and P. A. Lee, Localization and quantum-mechanical resonant tunneling in the presence of a time-dependent potential, Phys. Rev. B **31**, 1707 (1985).

[42] M. Abramowitz and A. Stegun, *Handbook of Mathematical Functions* (Dover Publications, New York, 1965).

[43] L. Buck and R. Axel, a novel multigene family may encode odorant receptors: A molecular basis for odor recognition, Cell **65**, 175 (1991).

[44] L. B. Buck, Olfactory receptors and odor coding in mammals, Nutr. Rev. **62**, S184 (2004); Science **286**, 701 (1999).

[45] B. Malnic, J. Hirono, T. Sato, and L. B. Buck, Combinatorial receptor codes for odors, Cell **96**, 713 (1999).

[46] R. B. Silverman, *The Organic Chemistry of Enzyme Catalyzed Reactions* (Academic Press/Elsevier, New York, 2002).

[47] S. Katada, T. Hirokawa, Y. Oka, M. Suwa, and K. Touhara, Structural basis for a broad but selective ligand spectrum of a mouse olfactory receptor: Mapping the odorant-binding site, J. Neurosci **25**, 1806 (2005).

[48] S. Longhi, Resonant tunneling in frustrated total internal reflection, Opt. Lett. **30**, 2781 (2005).

[49] M. Jazbinšek and M. Zgonik, Material tensor parameters of $LiNbO_3$ relevant for electro- and elasto-optics, Appl. Phys. B: Lasers Opt. **74**, 407 (2002).